Macromolecules

ARTICLE

pubs.acs.org/Macromolecules

Effect of Hyaluronan Solution on Dynamic Friction of PVA Gel Sliding on Weakly Adhesive Glass Substrate

Yukihiro Nakano,[†] Takayuki Kurokawa,[‡,§] Miao Du,[‡,⊥] Jian Liu,[†] Taiki Tominaga,[†] Yoshihito Osada,[‡] and Jian Ping Gong*[,‡]

[†]Graduate School of Science, Hokkaido University, Sapporo 060-0810, Japan

[‡]Faculty of Advanced Life Science, Hokkaido University, Sapporo 060-0810, Japan

[§]Creative Research Institution, Hokkaido University, Sapporo 060-0810, Japan

ABSTRACT: We study the sliding friction of poly(vinyl alcohol) (PVA) gel against glass substrate in hyaluronan (HA) aqueous solution with various concentrations and two molecular weights. The frictional stress decreases with increase of concentration of HA at low sliding velocity, and the lowest friction appears in HA $10c^*$ (c^* is the overlap concentration) solution; after that, it increases slightly with the concentration. By assuming that a continuous HA lubricant layer is formed at the interface, which screens PVA adsorption to substrate, we estimate the thickness of the lubrication film in concentrated HA solution. In addition, we perform frictional measurement in poly(ethylene oxide) (PEO) aqueous solutions and proteoglycan solutions. By comparing the frictional behavior with that in HA solutions, we observe a universal relationship between the zero-shear rate viscosity of polymer solution and the friction at low sliding velocity region, regardless the change in the lubricating polymer species.

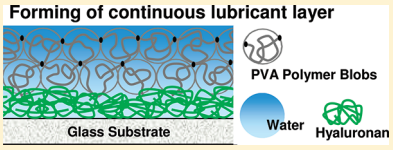

I. INTRODUCTION

There are many lubrication systems with various scales in human body. In these systems, many biopolymers, in hydrated state, work as lubricant as liquid and/or as adsorbed bottle brush. For example, human cornea is covered with mucus layer which consists of membrane-associated mucins,[1] and together with tears, it maintains eye−eyelid lubrication. A remarkable low friction system under high load is the joint. Mucins bound on the cartilage surface and synovial fluid, mainly containing hyaluronan with large molecular mass, act as lubricant.[2]

Inspired by these biological low friction systems, the friction of the sliding interfaces decorated with polymer brushes has been studied.[3−5] The remarkable low friction of such hairy polymer layers seems to be attributed to withstanding pressure of the brushes which containing large amount of solvent.

Another important character of the biolubrication system is that they usually adopt soft and wet materials to frictional surfaces like eyes, digestive tracts, and cartilages. Soft surfaces can deform elastically responding to external load and ease the local concentration of the pressure, which prevents the disruption of surface adsorbed polymers and breakage of the lubricant film.

In order to investigate the tribological properties of such soft and wet materials, sliding friction of various kinds of hydrogels has been investigated.[8−23] In a previous study, we investigated the friction behaviors of a soft neutral hydrogel, poly(vinyl alcohol) (PVA) gel, sliding against glass substrate in flexible polymer aqueous solution, poly(ethylene oxide) (PEO), which is nonadhesive to the substrate.[24] It has been found that PEO can effectively reduce the friction at low sliding velocity by screening the adhesive interfacial interaction between the PVA gel and the glass substrate.[24] The measurements, however, performed only for dilute PEO solution. Therefore, it is expected that the concentrated solution like synovial fluid sustains the normal load at soft interface and gives even larger lubrication effect than the dilute solution.

In this paper, we study the friction of physically cross-linked PVA gel on a glass substrate in sodium hyaluronate (HA) solution over dilute through concentrated regions. HA is a water-soluble glycosaminoglycane. Its primary structure consists of repeating disaccharide units of D-glucuronic acid and *N*-acetyl-D-glucosamine with $\beta(1-4)$ inter-glycosidic linkages. It exists in many living substances as synovial fluid, such as in articular cartilage, playing an important role in lubrication and maintaining the structural resistance of cartilage.[7] The effect of HA molecular weight, M_w, and concentration, c, on the frictional behavior of PVA gel is investigated. We further compare the lubrication behavior of HA with that of PEO and proteoglycan (PG) that is one of the two main components of cartilage.

II. EXPERIMENTS

Materials. PVA and PEO were produced by Wako Pure Chemical Industries, Ltd., and used without further purification. The degree of polymerization for PVA was 2000. The molecular weight of PEO was 4×10^6 g/mol, which is coded as PEO4E6. Dimethyl sulfoxide (DMSO) was provided by Junsei Chemical Co., Ltd., and used as solvent of PVA preparation without further purification. HA with different molecular weight was produced by Kibun Food Chemifa Co., Ltd., and used without further purification. The molecular weights of two kinds of HA were 9×10^4 and 2×10^6 g/mol, which are coded as HA 9E4 and HA 2E6, respectively. PG was produced by Biomatec Japan, Inc., and used without further purification. The molecular weight of PG was 2.7×10^6 g/mol.

Received: July 5, 2011
Revised: October 5, 2011
Published: October 21, 2011

Gel Preparation. Physically cross-linked PVA gel was prepared by a freezing (−40 °C) and thawing (25 °C) method, from a prescribed PVA solution (~10 wt % PVA, DMSO:H_2O = 67.5:22.5 w/w).[25] Solutions were prepared by heating PVA solution for 1 h at ~90 °C. After the heating step, the PVA solutions were placed in a dryer connecting with a vacuum pump to facilitate the release of air bubbles. When all air bubbles were removed, the solutions were cast between glass plates and quenched for 24 h at −40 °C. Following the quenching period, hydrogel sheets (~3 mm thick) were allowed to warm up to room temperature and then submerged in copious distilled water at least 1 week to extract DMSO. After removing DMSO, the PVA gel was put into a plenty of HA aqueous solutions of various concentration for 1 week to obtain equilibrium.

HA Solution. Sodium hyaluronate (HA) aqueous solutions containing 0.1 M NaCl to inhibit aggregation of HA and 0.2 g/L sodium azide for suppression of bacterial growth were prepared.

Measurements. The viscosity of HA solution was determined using a commercially available rheometer (ARES-100FRT) with a pair of parallel plates of 50 mm in diameter at 25 °C, covering a shear rate range from 10^{-2} to 10^{3} s^{-1}. The gap distance between the plates was 0.5−1.0 mm. The compressive modulus, E, of gels were measured by using tensile-compressive tester (TENSILON, ORIENTEC., Co.) at 25 °C. The cylindrical gel sample of 10 mm diameter and 2.6 mm thickness was set on the lower plate and compressed by the upper plate, which was connected to a load cell at a velocity of 10% in thickness/min. Since the gels used in this study were easily deformed, Hencky's strains (ε_h) and stresses (σ_h) were calculated, where ε_h and σ_h are the normal strain and stress, respectively. From the obtained relationship between ε_h and σ_h, we have calculated the modulus of compressive elasticity of each gel at a strain of less than 10%. E of PVA gel in HA solution were measured after immersed in the solution for 1 week.

The friction force of PVA gel against a glass substrate in pure water or in HA aqueous solution at 20 °C was performed using a rheometer (ARES-2KFRT, Rheometric Scientific Inc.) that works in a constant compressive strain mode. The swollen PVA gel, 2.6 mm in thickness, soaked in copious HA aqueous solution for 1 week, was cut into a disk shape of 15 mm in diameter and then was glued on the upper surface of coaxial disk-shaped platen of rheometer with cyanoacrylate instant adhesive agent (Toa Gosei Co., Ltd.). The glass substrate, square shape of 25 mm in side, was glued onto the lower platen of rheometer. The separated gel−glass interface was immersed in pure water or HA aqueous solution at a prescribed temperature and equilibrated for 20 min, and then the PVA gel was allowed to approach to glass surface at a velocity of 2 μm/s until the normal load increased to 14 kPa.

Steady rate sweep test (SRST) mode measurements were performed after the normal strain was applied for 15 min, whereupon an angular displacement was applied to the lower platen at a constant angular velocity (ω). The angular velocity dependence at a certain experimental condition was studied by steady rate sweeping changes without separating the two rotating surfaces in the velocity change from lower to higher values. ω was increased stepwise from 10^{-3} to 10 rad/s for 40 s at each rotating velocity. The average torque T of last 20 s was adopted. No stick−slip was observed, and each friction in the last 20 s reached almost constant even for the lowest velocity. The frictional stress adopted in figures was the average of three different measurements, and the standard deviation of the data was less than 30% except the 10c^* solution that was slightly high (less than 50%).

The frictional force, F, was calculated as $F = 4T/3R$, where T was the frictional torque recorded during measurement and R (=7.5 mm) was the radius of the apparent contact area. The average frictional shear stress, σ, generated at the interface was qualified as the friction force per unit area, $\sigma = F/\pi R^2$. Although the sliding velocity varies along the radial direction in parallel plate geometry, we used the sliding velocity v at the outer side of disk-shape samples, $v = \omega R$.

Table 1. Estimated Overlap Concentration c^*, Radius of Gyration of Random Coil R_g, Osmotic Pressure at c^*, π^*, and Osmotic Pressure by Donna Effect, π^*_{ion}, for HA with Two Molecular Weight, M_w

HA sample	M_w [g/mol]	c^* [g/L]	R_g (nm)	π^* (Pa)	π^*_{ion} (Pa)
HA 9E4	90 000	2.03	26.0	2.34×10^2	1.57×10^2
HA 2E6	2 120 000	0.260	148	1.27	2.58

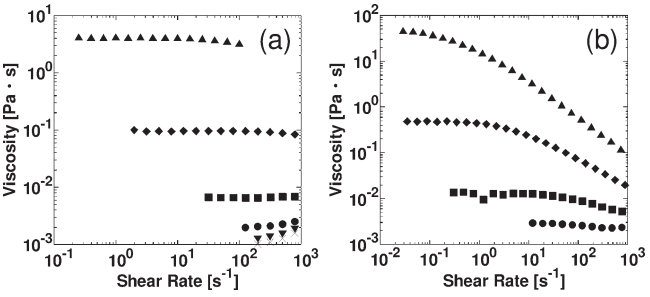

Figure 1. Dependence of viscosity on shear rate for HA solutions of different molecular weights at 25 °C. (a) HA 9E4; (b) HA 2E6. Scaled concentration of HA c/c^*: (×) 0.1, (▼) 0.3, (●) 1.0, (■) 3.0, (◆) 10, and (▲) 30.

III. PROPERTIES OF HA AQUEOUS SOLUTION AND PVA GEL

Solution Properties of HA. The crossover concentration c^* is related to the molecular weight M_w of HA as[26]

$$c^* = \{(4/3)\pi R_g^3 N_A M_w\}^{-1} \times 10^3 \text{ (g/L)} \quad (1)$$

where N_A is the Avogadro constant. R_g is the radius gyration of HA randam coil, described as[26]

$$R_g = K' M_w^{\nu} \quad (2)$$

In the range $4 \times 10^5 < M_w < 1.5 \times 10^6$ and in the SEC conditions (0.1 M $NaNO_3$, 30 °C), K' and ν were experimentally determined as 0.049 and 0.55, respectively.[26] In other SEC conditions (0.15 M NaCl, 37 °C) within a broader range $4 \times 10^4 < M_w < 5.5 \times 10^6$, K' and ν were 0.0275 and 0.596, respectively.[27] Whatever the values are used, it makes little difference in R_g when M_w is 9×10^4 and 2×10^6 g/mol. Using eqs 1 and 2, and the former K' and ν, R_g and c^* of HA with two molecular weight are calculated, shown in Table1. It reveals that the real concentration of c^* solution of HA 2E6 is about 10 times lower than that of HA 9E4 due to its high molecular weight.

Figure 1 depicts the shear rate dependence of the viscosity for HA aqueous solutions with different molecular weight and concentration. For HA 9E4 solution of all concentrations, no shear thinning is observed in the measurement region, where shear rate, $\dot{\gamma}$, is from 0.1 to 1000 s^{-1}. For HA 2E6, however, the shear thinning appears even for semidiluted concentration. For example, shear thinning appears when $\dot{\gamma}$ is 10 and 1 s^{-1} for HA 2E6 3c^* and 10c^* solution, respectively. Figure 2 shows double-logarithmic plots of the zero-shear rate viscosity η_0 vs c/c^* for HA 9E4 and HA 2E6 solutions. η_0 is nicely scaled by c/c^* regardless the huge differences in molecular weight of HA. The viscosity η_0 increases slightly with an increase in c/c^* in the region $c/c^* < 1$, while at $c/c^* > 10$, the viscosity increases intensively with a scaling

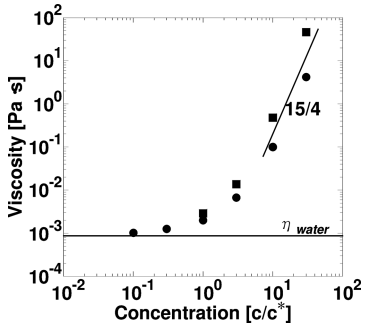

Figure 2. Relationship between zero-shear-rate viscosity and scaled concentration c/c^* of HA solutions at 25 °C: (●) HA 9E4; (■) HA 2E6. The slope 15/4 indicates the theoretical value.

relationship of $\eta \propto (c/c^*)^{15/4}$. These behaviors are basically in agreement with the theoretical relationships that $\eta_0 \propto \eta_s(1 + \phi)(c/c^* \ll 1)$ and $\eta \propto (c/c^*)^{15/4}(c/c^* > 10)$ for neutral polymer solution, where ϕ is the polymer volume fraction and η_s is the solvent viscosity.[28,29] This result indicates that HA solution used in the present study has a well-defined rheological behavior as linear polymers.

Effect of HA Solution on Elasticity and Swelling Degree of PVA Gel. As has been described in our previous work, when gels are immersed in a polymer solution that has no specific molecular interaction with each other, two effects might occur: (1) diffusion of soluble polymer chains into gel networks; (2) deswelling of gels by the osmotic pressure of polymer solution.[24]

Regarding the first effect, the diffusion kinetics of polymer chain into a network is characterized by the radius of gyration, R_g, to the mesh size of the network, ξ. When $R_g \ll \xi$, the diffusion is in translational mode. When $R_g \gg \xi$, the diffusion is in reputational mode.[28] From Table1, we know that R_g of HA molecule is 26 and 145 nm for HA 9E4 and HA 2E6, respectively, larger than the mesh size of PVA gel that is in the order of several nanometers. The latter can be estimated from the scaling relation, $G \cong k_BT/\xi^3$, where G is the shear modulus of the gel and k_B and T have their usual meaning.[28] So translational diffusion of HA random coil into PVA gel can be neglected. HA may penetrate into the gel by reptation mode that will take a prolonged time.

Next, we consider the osmotic effect of HA solutions on PVA gels using the results of scaling theory. In dilute neutral polymer solution $(c/c^* \leq 1)$, the osmotic pressure π is related to the polymer concentration c in terms of osmotic pressure of solution at c^*, $\pi^* \cong k_BT/R_g^3$ as follows:[24]

$$\pi \cong \pi^*\left[\frac{c}{c^*}\right] \quad (c/c^* \leq 1) \tag{3}$$

In semidilute and concentrated solution $(c/c^* > 1)$

$$\pi \cong \pi^*(c/c^*)^{9/4} \quad (c/c^* > 1) \tag{4}$$

In addition, since HA is a polymer with negative charge, osmotic pressure by the Donna effect, π_{ion}, must be considered. It is described as[30]

$$\pi_{ion} \cong RTC_{NaCl}(Y + Y^{-1} - 2) \tag{5}$$

where R is gas constant, T is the temperature, C_{NaCl} is concentration of NaCl, and Y is ratio of sodium ion concentration between inside and outside of gel.

$$Y = -\frac{zC_{HA}}{2C_{NaCl}} + \sqrt{1 + \left(\frac{zC_{HA}}{2C_{NaCl}}\right)^2} \tag{6}$$

where z is charge number of one HA molecule and C_{HA} is concentration of HA molecule. So zC_{HA} is the concentration of charges of HA. Using eqs 3−6, the total osmotic pressure $\pi_{total} = \pi + \pi_{ion}$ is calculated and shown in Figure 3. The osmotic pressures at c^* concentration are also shown in Table 1. From Figure 3, the total osmotic pressure π_{total} at dilute and semi dilute solution is much less than the elastic modulus G (G is one-third of the Young's modulus E = 70 kPa) of the PVA gel in pure water and will not deswell the gel.

However, in the concentrated HA solution, for example, at $c/c^* = 10$, the osmotic pressure π_{total} for HA 9E4 and HA 2E6 are estimated as 57 and 2.5 kPa, respectively. The former is comparable to the elastic modulus G of the gel, so the gel will deswell at the equilibrium state. The molecular weight effect on the osmotic pressure is clearly observed in the swelling degree change of PVA gels in the HA solutions. Figure 4 depicts the experimentally determined relation between the swelling degree (q) (Figure 4a) or Young's modulus (E) (Figure 4b) of PVA gel and the concentration (c/c^*) of HA solution for HA 9E4 and HA 2E6.

For comparison, q and E of PVA in 0.1 M NaCl solution are also shown in the figure. As shown in Figure 4a, the gel does not change in its swelling degree q over the whole concentration range when being immersed in the HA 2E6 solutions for 2 months (which is assumed to be in equilibrium swelling state). On the other hand, the gel exhibits a distinct deswelling in HA 9E4 solutions at the high concentration region ($c/c^* > 3$). These behaviors are in agreement with the estimation of the osmotic pressure of HA solution exerted on the gels. As shown in Figure 4b, PVA does not show a change in Young's modulus E in HA 2E6 solutions within the experimental accuracy, while in HA 9E4 of the high concentration, the gel shows an increase in E. The results for E values are in agreement with the results in q values. Actually, it is confirmed that E and q follow the scaling relationship of $E \propto q^{-3}$ for a neutral gel in good solvent.[28] Since a change of swelling degree and Young's modulus will cause change in the frictional behavior, we try to avoid this change by performing the frictional measurements after immersing the gel in the HA solution for 1 week that is short enough to cause any change in the q and the E values. As shown in Figure 4b, even in the HA 9E4 of the high concentration ($c/c^* > 1$), E does not change largely within 1 week. This ensure us to discuss the HA effect on the PVA friction over a wide concentration range while keeping q and E constant.

IV. FRICTION OF PVA GEL IN HA SOLUTION

Results by SRST Mode. Figure 5 gives the friction behavior of PVA gel against glass surface in various HA solutions under a normal pressure of 14 kPa. In the low-velocity region, the frictional stress dramatically decreases with the increase in the HA concentration, and the lowest friction appears in HA 10c^* solution (Figure 5a); after that, it increases slightly with the concentration, although the zero-shear rate viscosity of the fluid increases more than 3 orders of magnitude with the increase of HA concentration from 0 to 30c^*, as shown in Figure 2. However, with the increase of sliding velocity, the effect of HA on friction

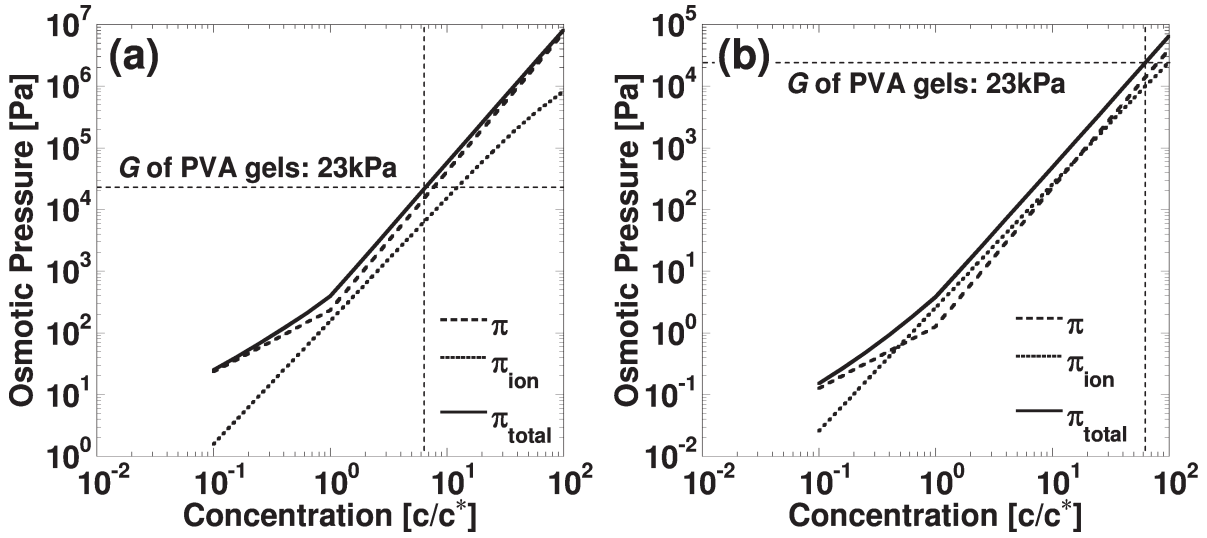

Figure 3. Estimated relationships between the scaled concentration (c/c^*) of HA solutions of two different molecular weights and the osmotic pressures from polymer chains π, counterions π_{ion}, and the total osmotic pressure ($\pi_{total} = \pi + \pi_{ion}$) exerted on PVA gels. The elastic modulus G of PVA gel is also shown in the figures. (a) HA 9E4; (b) HA 2E6.

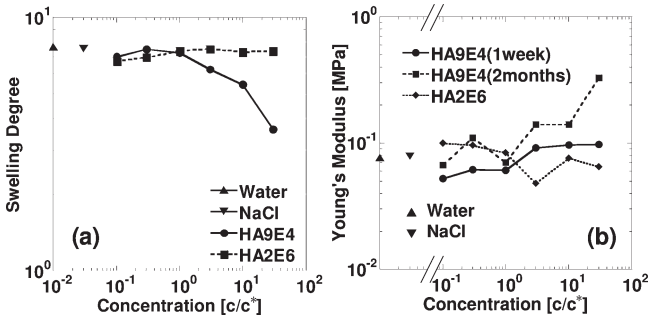

Figure 4. Swelling degree (a) and Young's modulus (b) of PVA gel in HA solutions of various concentrations. For comparison, the results in pure water and 0.1 M NaCl solution are also shown.

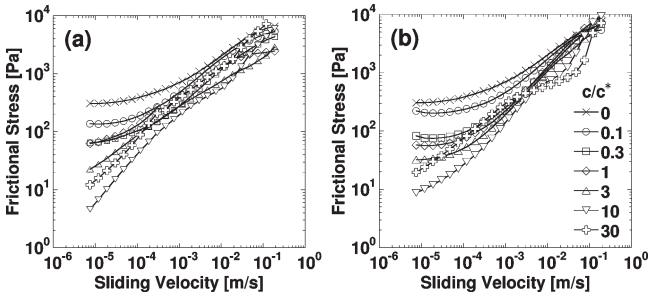

Figure 5. Sliding velocity dependence of the frictional stress of PVA gels against glass substrate in HA solution of various concentrations. Normal pressure: 14 kPa. (a) HA 9E4; (b) HA 2E6.

diminishes, and all the friction curves converge to the friction curve in pure water at velocities higher than 10^{-2} m/s. Similar behavior is observed for HA 2E6, as shown by Figure 5b.

In Figure 6, frictional stress is plotted against the HA concentration c/c^* (Figure 6a) and against the HA zero-shear rate viscosity (Figure 6b), at the lowest sliding velocity (v = 7.5 × 10^{-6} m/s). The figure clearly shows that the frictional stress dramatically decreases with the increase in the HA concentration,

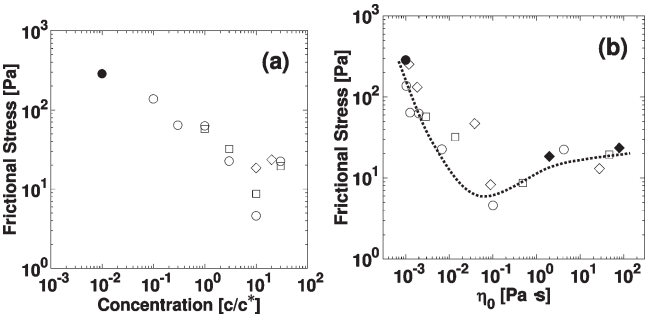

Figure 6. Dependence of the frictional stress of PVA gels on HA concentration c/c^* (a) and on zero shear rate viscosity of HA (b) at a low sliding velocity (7.5 × 10^{-6} m/s). For comparison, the results in PEO 4E6 and in PGs are also shown in the figure. (○) HA 9E4, (□) HA 2E6, (●) water, (◆) PGs, (◇) PEO 4E6 (1.15 × 10^{-5} m/s).

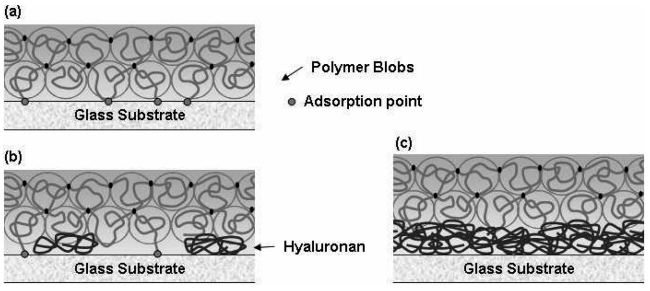

Figure 7. Illustration of frictional interface: (a) in water; (b) in dilute and semidilute solution ($c/c^* < 10$); (c) in concentrated solution ($c/c^* > 10$).

reaching a minimum at the zero-shear rate viscosity of 0.1 Pa·s, corresponding to $10c^*$, and then gradually increases, regardless of the dramatic increase in the viscosity.

This viscosity effect does not change with the molecular weight. The remarkable decrease in the friction with the increase in the HA concentration below $10c^*$ can be understood by the screening of the gel adsorption to the substrate by HA molecules (Figure 7b).

dx.doi.org/10.1021/ma201522q |*Macromolecules* 2011, 44, 8908–8915

The increase of frictional stress above $10c^*$ indicates the formation of continuous lubricant film and the fluid resistance of HA increases with the viscosity of the HA (Figure 7c).

It should be pointed out that the minimum frictional stress, which means the maximum lubrication effect by the HA, is observed around $10c^*$ though a complete screening of the gel—substrate adhesion should be accomplished at c^* since at the c^* concentration, HA molecules start to overlap with each other and the interface is already filled with HA. This phenomenon can be understood as follows. Because HA molecules are always fluctuating and there is no specific interaction between HA and PVA, PVA polymer chains can make contact and adsorption to glass substrate through the molecule fluctuation even when HA is higher than c^* in the semidilute solution in which HA molecules are still not entangled. However, HA lubricant molecules form strong entanglement in concentrated solution and the adsorption of PVA to the substrate is completely screened.

Estimation of Lubricant Film Thickness. We assume that the dramatic decrease of the frictional stress in HA solutions is due to intervene of HA between frictional interfaces, which serves as a fluid lubricant layer. Above $10c^*$, no direct contact of PVA gel on substrate, and friction is due to the viscous lubrication of the HA polymer. So, we try to calculate the thickness of lubricant film h, assuming that the frictional stress σ is originated from fluid lubrication. In principle, we can obtain the shear rate $\dot{\gamma}$ exerted on the lubrication film from the experimentally determined rheogram $\tau \sim \dot{\gamma}$, supposing that the frictional stress σ equals to the shear stress τ of viscous polymer solution. Then the sliding velocity in Figure 5 is related to $\dot{\gamma}$ through eq 7, and the film thickness h can be calculated.

$$\dot{\gamma} = \frac{v}{h} \tag{7}$$

In reality, however, the shear rate exerted on the lubricant film at high sliding velocity region is higher than the high shear rate limitation of viscometry, as can be seem from the high frictional stress σ in this region. So we need extrapolation of rheograms to higher shear rate regions beyond the experimental limitation. The shear stress τ of viscous polymer solution at high shear rate $\dot{\gamma}$ is related to $\dot{\gamma}$ by Casson's equation[31]

$$\sqrt{\tau} = k_0 + k_1\sqrt{\dot{\gamma}} \tag{8}$$

k_0 and k_1 are constants, depending on the polymers and their concentrations. k_0 and k_1 are determined by experimentally measure the relationship between τ and $\dot{\gamma}$ of the polymer at various concentrations around the measurement limitation at the high shear rate.

Figure 8 shows sliding velocity dependence of lubricant film thickness h for HA 2E6 estimated from the extrapolated rheograms by using eq 8, k_0 and k_1.

At low sliding velocity, the estimated thickness of lubricant film is much smaller than the radius of gyration of HA 2E6 molecule below $10c^*$ concentration, which indicates that a continuous lubricant film is not formed, and the h values estimated has no physical meaning. Therefore, the effect of friction reduction of HA is considered to be due to partial screening of the gel adsorption to the substrate by HA molecules in low HA concentrations ($c < 10c^*$), and the friction is from two contributions: gel adhesion and partial lubrication. In concentrated $30c^*$ HA solution at low sliding velocity, extremely thick film seems to be formed. So it is in consistent with the assumption that the gel has no direct contact with the substrate, and a continuous lubricant film is formed at the interface. The friction at this concentration is due to lubrication of the polymer layer.

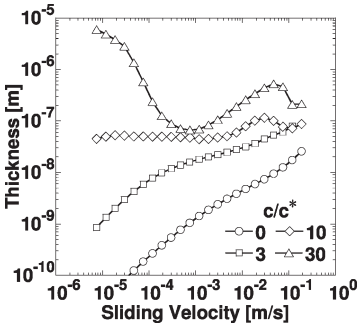

Figure 8. Dependence of the estimated lubricant film thickness on sliding velocity for PVA gel friction in HA 2E6 solutions. The thickness at low sliding velocity region for $c/c^* = 0$ and 3 become less than nanometer order, indicating that no continuous lubricant layer is formed and the thickness thus estimated has no physical meaning in these conditions.

In high sliding velocity, the calculated thickness of lubricant film becomes as large as the size of the HA 2E6 molecule even in dilute solutions, and it indicates that friction changed to fluid lubrication. In addition, the thicknesses converge to constant value. It means that the viscosity of the lubricant film decreases to that of water with increase of shear rate.

It should be pointed out that even at the lowest sliding velocity($v = 7.5 \times 10^{-6}$ m/s) shear thinning already occurs, as can be clarified by comparing the frictional stress σ in Figure 5 with the shear stress τ using the relation $\tau = \eta\gamma$ in Figure 1. Therefore, at $c = 10c^*$, though the lubrication film thickness is about 40 nm that is smaller than the radius of gyration of HA 2E6 molecule (145 nm), homogeneous lubricant film might be formed over the whole velocity range considering that HA molecule is pressed and stretched by the shear.

For HA 9E4 which has a short molecular weight, shear thinning could not be observed in the measurement range (Figure 1a), but it is expected to occur under higher shear rate. It is considered that extrapolation of the rheogram from flat region would not give the correct value, so we did not perform the estimation of lubricant film thickness for HA 9E4.

HA Molecules Confined between Frictional Surfaces. From the results shown in Figure 8, the lubricant film thickness in dilute solution ($c/c^* < 10$) is much smaller than the size of a polymer coil R_g at low sliding velocity, indicating a boundary lubrication mechanism. Here we discuss the HA chain confinement and conformation at the interface, which can be treated as a problem of polymer chain confinement between a pair of plates with distance D ($D/R_g < 1$) for dilute solution. According to our previous paper, the polymer concentration c^i in such a confined space is related to the bulk concentration c as follows:[24]

$$c^i \cong c\left(\frac{R_g}{D}\right) \tag{9}$$

Thus, the osmotic pressure π^i due to the polymer chain in the confined space is[24]

$$\pi^i \cong \pi\left[\frac{R_g}{D} + \frac{5}{3}\left(\frac{R_g}{D}\right)^{8/3}\right]$$

$$= \pi_1^i + \pi_2^i \quad \left(\pi_1^i = \frac{R_g}{D},\ \pi_2^i = \frac{5}{3}\left(\frac{R_g}{D}\right)^{8/3}\right) \tag{10}$$

Furthermore, the osmotic pressure by Donna effect, π_{ion}^i, is determined by eq 6, where the HA concentration in the confined

space $C^i_{HA} = C_{HA}(R_g/D)$, that is

$$\pi^i_{ion} \cong RTC_{NaCl}(Y + Y^{-1} - 2) \quad (11)$$

$$Y = -\frac{zC_{HA}(R_g/D)}{2C_{NaCl}} + \sqrt{1 + \left(\frac{zC_{HA}(R_g/D)}{2C_{NaCl}}\right)^2} \quad (12)$$

Then the total osmotic pressure from the confinement of polymer, $\pi^i_{total} = \pi^i_1 + \pi^i_2 + \pi^i_{ion}$. Figure 9 shows the dependence of π^i_1, π^i_2, π^i_{ion}, and π^i_{total} on R_g/D. Figure 9 indicates that π^i_2 is predominant when the external normal pressure P (=14 kPa) is balanced by π^i_{total}, so using the equilibrium condition, $P = \pi^i_2 = (5/3)(R_g/D)^{8/3}$, we can estimate the D. Results are shown in Table 2.

In dilute solution, the estimated D is smaller than the persistence length L_p of HA molecule, 9 nm.[25] Therefore, in such strong confinement, HA molecule could no longer be treated as a coil made of flexible chain, and there is little degree of freedom of the molecular movement.[31] Because of the charge screening of HA by NaCl, there is no specific interaction between HA and glass substrate. In this strong confinement, HA molecules might repeat weak absorption and desorption depending on shear or friction; they are dragged by surface shear stress.

Because D is almost equal to L_p in c^* HA solution, D is expected to be larger than L_p in $3c^*$ HA solution. In this moderately confined regime, HA molecules are confined substantially but still behave as flexible chains.[31]

As shown by Figure 8, the lubricant film thickness in concentrated solution ($c/c^* = 30$) is larger than the size of a polymer coil R_g at low sliding velocity, indicating a hydrodynamic lubrication mechanism. Though there is no direct information on molecular conformation in the concentrated solution, the HA molecules might behave as flexible chains because the calculated lubricant film thickness is larger than R_g. Because of the high shear rate exerted on the lubricant, it is expected that HA molecules are substantially oriented in the direction of shear, and the real viscosity is much lower than the zero-shear viscosity η_0. To confirm the behavior of the confined lubricant, direct observation of frictional interfaces is required using possible approaches such as the polarizing microscopy, tracking of fluorescently labeled molecules. These should be performed in future study.

V. FRICTION OF PVA GEL IN PEO AND PG SOLUTIONS

Results by SRST Mode. In a previous work, we have studied the friction of PVA gels in PEO 2E4 and PEO 4E6 solution in a dilute concentration range of $0-c^*$ and have found that dilute PEO solution has a similar friction reduction effect as HA at the low-velocity region.[24] To make a more systematic comparison of HA with PEO, we further study the PVA friction in PEO 4E6 over dilute through concentrated regions. As shown in Figure 10, though the frictional behavior in dilute PEO 4E6 solutions is different from that in HA solutions, the frictional behavior in concentrated PEO 4E6 solutions ($>10c^*$) at low sliding velocity is similar to that in HA 2E6 solutions of the similar molecular weight (Figure 5b).

Additionally, we have studied the lubrication effect of branched polymer, proteoglycan (PG), which has almost the same molecular weight as HA 2E6. For comparison, we also plot the results of PEO and PG in the same figure (Figure 6). We found that friction at low sliding velocity shows a similar dependence on

Table 2. Estimated Confined Thickness D for HA 9E4 and HA 2E6 in Dilute Solution[a]

HA 9E4				HA 2E6			
c/c^*	D (nm)	D/R_g	D/L_p	c/c^*	D (nm)	D/R_g	D/L_p
0.1	2.9	0.11	0.33	0.1	2.5	0.017	0.27
0.3	4.6	0.18	0.51	0.3	4.2	0.028	0.46
1	8.2	0.32	0.91	1	8.3	0.056	0.92

[a] L_p is the persistence length of HA molecule.

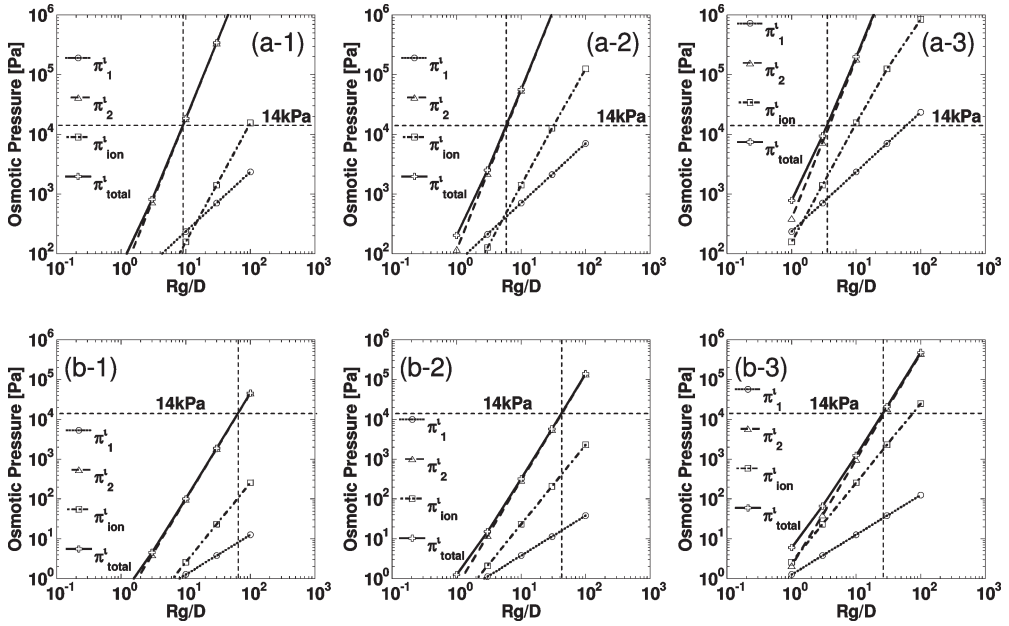

Figure 9. Dependence of π^i_1, π^i_2, π^i_{ion}, and π^i_{total} on R_g/D: (a-1) HA 9E4 $0.1c^*$, (a-2) HA 9E4 $0.3c^*$, (a-3) HA 9E4 $1c^*$, (b-1) HA 2E6 $0.1c^*$, (b-2) HA 2E6 $0.3c^*$, (b-3) HA 2E6 $1c^*$. π^i_2 is predominant when π^i_{total} is equal to external normal pressure P, 14 kPa.

dx.doi.org/10.1021/ma201522q |Macromolecules 2011, 44, 8908–8915

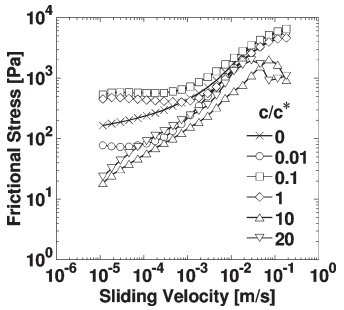

Figure 10. Sliding velocity dependence of the frictional stress of PVA gels in PEO 4E6 solution. Normal pressure: 14 kPa.

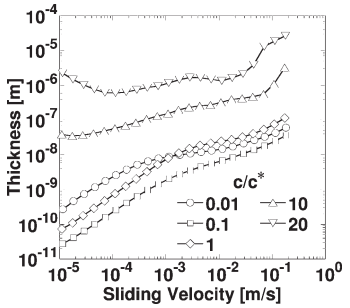

Figure 11. Dependence of the estimated hydrodynamic lubricant film thickness on sliding velocity for PVA gel friction in PEO 4E6 solution. The thickness at low sliding velocity region for $c/c^* = 0.01, 0.1, 1$ become less than nanometer order, indicating that no continuous lubricant layer is formed and the thickness has no physical meaning in these conditions.

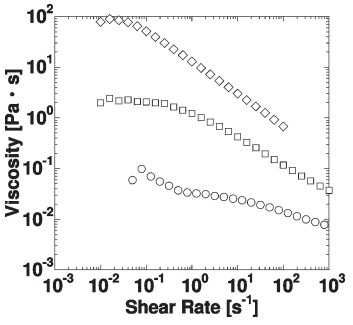

Figure 12. Dependence of viscosity on shear rate for PEO solution at 25 °C. Scaled PEO concentration c/c^*: (○) 3.0; (□) 10; (◇) 30.

the viscosity of lubricants and does not depend on the polymer species. This result indicates that fluid resistance of lubricants dominates the frictional stress in concentrated polymer solutions.

Because of having the similar viscous behavior, in the same way as HA, lubricant film thickness of PEO solutions is calculated. From Figure 11, the thickness is nearly equal to that of HA at low sliding velocity in concentrated region ($10c^*$, $20c^*$). On the other hand, PEO keep thick lubricant film ($\sim$0.6 μm) over the whole sliding velocity. It indicates different shear response of polymers, and it can be considered that flexibility of molecule, molecular weight, and interactions of the polymers with the substrate are responsible for the difference.

VI. CONCLUSIONS

The relationship of frictional stress and sliding velocity about PVA gel friction against glass in various HA solutions was studied by a strain-controlled rheometer. Frictional stress decreases with increase of HA concentration, and the lowest value appears in HA $10c^*$ solution; after that, it increases slightly with the concentration, independent of the molecular weight. The friction reduction effect of HA solution is large, especially at low sliding velocity, and the frictional stress in concentrated HA solutions is lower than a tenth of that in water. The frictional stress increases with increase of sliding velocity, and the difference in frictional stress attributed to concentration becomes smaller at the high-velocity region.

Assuming that gel friction is due to fluid lubrication, the hydrodynamic lubricant film thickness was calculated. Lubricant film becomes thicker with increase of HA concentration, and it appears that continuous lubricant film is formed over the whole measuring velocity in HA $30c^*$.

Not only HA but also PEO and PG show the same lubrication effects on PVA gel friction against glass substrate at low sliding velocity. It suggests that this lubrication effect of hydrophilic polymers on hydrogel friction is universal and only depends on the rheological properties of the polymer. This result also suggests that the lubrication effect of HA in human body such as in joints is not due to its specific structure but due to its polymeric nature. Meanwhile, properties of hydrogels, high wettability, and softness support the lubrication effect of polymer solutions. It suggests the potential for various kinds of polymers including not only biopolymer but also synthetic polymers to serve as biolubricant like eye drops and joint fluid. At the same time, it also indicates that synthetic hydrogels like PVA gel have potency for artificial organs which enable smooth movement and low abrasion property.

AUTHOR INFORMATION

Corresponding Author

*Tel +81 11 706 2774; fax +81 11 706 2774; e-mail gong@sci.hokudai.ac.jp.

Present Addresses

⊥Department of Polymer Science and Engineering, Zhejiang University, P. R. China.

ACKNOWLEDGMENT

This work is supported by a Grant-in-Aid for the Specially Promoted Research (No. 18002002) from the Ministry of Education, Science, Sports and Culture of Japan. Authors thank Marguerite Rinaudo for her helpful discussions.

REFERENCES

(1) Gipson, I. K. *Exp. Eye Res.* **2004**, *78*, 379–388.
(2) Bansil, R.; Stanley, E.; LaMont, J. T. *Annu. Rev. Physiol.* **1995**, *57*, 635–657.
(3) Raviv, U.; Giasson, S.; Kampf, N.; Gohy, F. J.; Jerome, R.; Klein, J. *Nature* **2003**, *425*, 163–165.
(4) Klein, J.; Kumacheva, E.; Mahalu, D.; Perahia, D.; Fetters, L. J. *Nature* **1994**, *370*, 634.
(5) Yan, X.; Perry, S. S.; Spencer, N. D.; Pasche, S.; Paul, S. M.; Textor, M.; Lim, M. S. *Langmuir* **2004**, *20*, 423–428.
(6) Fung, Y. C. *Biomechanics: Mechanical Properties of Living Tissues*, 2nd ed.; Springer-Verlag: New York, 1993.

(7) Gong, J. P.; Higa, M.; Iwasaki, Y.; Katsuyama, Y.; Osada, Y. *J. Phys. Chem. B* **1997**, *101*, 5487.
(8) Gong, J. P.; Osada, Y. *J. Chem. Phys.* **1998**, *109*, 8062.
(9) Gong, J. P.; Iwasaki, Y.; Osada, Y.; Kurihara, K.; Hamai, Y. *J. Phys. Chem. B* **1999**, *103*, 6001.
(10) Gong, J. P.; Kagata, G.; Osada, Y. *J. Phys. Chem. B* **1999**, *103*, 6007.
(11) Gong, J. P.; Iwasaki, Y.; Osada, Y. *J. Phys. Chem. B* **2000**, *104*, 3423.
(12) Gong, J. P.; Kurokawa, T.; Narita, T.; Kagata, K.; Osada, Y.; Nishimura, G.; Kinjo, M. *J. Am. Chem. Soc.* **2001**, *123*, 5582.
(13) Kagata, G.; Gong, J. P.; Osada, Y. *J. Phys. Chem. B* **2002**, *106*, 4596.
(14) Kurokawa, T.; Gong, J. P.; Osada, Y. *Macromolecules* **2002**, *35*, 8161.
(15) Baumberger, T.; Caroli, C.; Ronsin, O. *Phys. Rev. Lett.* **2002**, *88*, 75509.
(16) Kagata, G.; Gong, J. P.; Osada, Y. *J. Phys. Chem. B* **2003**, *107*, 10221.
(17) Baumberger, T.; Caroli, C.; Ronsin, O. *Eur. Phys. J. E* **2003**, *11*, 85.
(18) Ohsedo, Y.; Takashina, R.; Gong, J. P.; Osada, Y. *Langmiur* **2004**, *20*, 6549.
(19) Tada, T.; Kaneko, D.; Gong, J. P.; Kaneko, T.; Osada, Y. *Tribol. Lett.* **2004**, *17*, 505.
(20) Kaneko, D.; Tada, T.; Kurokawa, T.; Gong, J. P.; Osada, Y. *Adv. Mater.* **2004**, *17*, 535.
(21) Kurokawa, T.; Tominaga, T.; Katsuyama, Y.; Kuwabara, R.; Furukawa, H.; Osada, Y.; Gong, J. P. *Langmiur* **2005**, *21*, 8643.
(22) Nitta, Y.; Haga, H.; Kawabata, K. *J. Phys. IV* **2002**, *12*, 319.
(23) Miao, D.; Maki, Y.; Tominaga, T.; Furukawa, H.; Gong, J. P.; Osada, Y.; Zheng, Q. *Macromolecules* **2007**, *40*, 4313–4321.
(24) Trieu, H.; Qutubuddin, S. *Polymer* **1995**, *36*, 2531.
(25) Milas, M. *Polysaccharides: Structural Diversity and Functional Versatility*, 2nd ed.; Severian, D., Ed.; CRC Press: New York, 2005.
(26) Mendichi, R.; Šoltés, L.; Schieroni, A. G. *Biomacromolecules* **2003**, *4*, 1805–1810.
(27) De Gennes, P. G. *Scaling Concept in Polymer Physics*; Cornell University Press: Ithaca, NY, 1979.
(28) Doi, M.; Edwards, S. F. *The Theory of Polymer Dynamics*; Claredon Press: Oxford, 1986.
(29) Eisenberg, D. *Physical Chemistry: With Applications to the Life Sciences*; Addison Wesley Longman: Boston, MA, 1979.
(30) Casson, N. *Rheology of Dispersion Systems*; Pergamon Press: London, 1959.
(31) Graham, M. D. *Annu. Rev. Fluid Mech.* **2011**, *43*, 273–298.